



Intra-abdominal laparoscopic assessment of organs perfusion using imaging photoplethysmography

Victor A. Kashchenko^{1,2} · Alexander V. Lodygin^{1,2} · Konstantin Yu. Krasnoselsky^{1,3} · Valeriy V. Zaytsev^{4,5} · Alexei A. Kamshilin^{4,5}

Received: 28 July 2023 / Accepted: 23 September 2023 / Published online: 23 October 2023
© The Author(s), under exclusive licence to Springer Science+Business Media, LLC, part of Springer Nature 2023

Abstract

Background An objective evaluation of the functional state and viability of biological tissues during minimally invasive surgery remains unsolved task. Various non-contact methods for evaluating perfusion during laparoscopic surgery are discussed in the literature, but so far there have been no reports of their use in clinical settings.

Methods and patients Imaging photoplethysmography (iPPG) is a new method for quantitative assessment of perfusion distribution along the tissue. This is the first study in which we demonstrate successful use of iPPG to assess perfusion of organs during laparoscopic surgery in an operation theater. We used a standard rigid laparoscope connected to a standard digital monochrome camera, and abdominal organs were illuminated by green light. A distinctive feature is the synchronous recording of video frames and electrocardiogram with subsequent correlation data processing. During the laparoscopically assisted surgeries in nine cancer patients, the gradient of perfusion of the affected organs was evaluated. In particular, measurements were carried out before preparing a part of the intestine or stomach for resection, after anastomosis, or during physiological tests.

Results The spatial distribution of perfusion and its changes over time were successfully measured in all surgical cases. In particular, perfusion gradient of an intestine before resection was visualized and quantified by our iPPG laparoscope in all respective cases. It was also demonstrated that systemic administration of norepinephrine leads to a sharper gradient between well and poorly perfused areas of the colon. In four surgical cases, we have shown capability of the laparoscopic iPPG system for intra-abdominal assessment of perfusion in the anastomosed organs. Moreover, good repeatability of continuous long-term measurements of tissue perfusion inside the abdominal cavity was experimentally demonstrated.

Conclusion Our study carried out in real clinical settings has shown that iPPG laparoscope is feasible for intra-abdominal visualization and quantitative assessment of perfusion distribution.

Keywords Clinical evaluation study · Laparoscopic surgery · Intraoperative perfusion assessment · Imaging photoplethysmography · Gastrointestinal surgery · Minimally invasive surgery

✉ Alexei A. Kamshilin
alexei.kamshilin@yandex.ru

¹ First Surgical Department, North-Western District Scientific and Clinical Center Named After L.G. Sokolov of the Federal Medical and Biological Agency, Saint Petersburg, Russia 194291

² Department of Faculty Surgery, St. Petersburg State University, Saint Petersburg, Russia 199106

³ Department of Anesthesiology-Resuscitation and Emergency Pediatrics, St. Petersburg State Pediatric Medical University, Saint Petersburg, Russia 194100

⁴ Laboratory of New Functional Materials for Photonics, Institute of Automation and Control Processes of the Far Eastern Branch of the Russian Academy of Sciences, Vladivostok, Russia 690041

⁵ Organizational and Methodological Department, North-Western District Scientific and Clinical Center Named After L.G. Sokolov of the Federal Medical and Biological Agency, Saint Petersburg, Russia 194291

Laparoscopically assisted surgery has low invasiveness and significantly reduces the time of subsequent recovery of the patient. Intraoperative assessment of intestinal perfusion plays a primary role in making surgical decisions when performing reconstructive intestinal resections [1]. If perfusion could be monitored and quantified during the laparoscopic stage of surgery, the surgeon could change the reconstructive design at the earliest stage. However, during standard laparoscopy, an objective intraoperative assessment of the functional state and viability of biological tissues remains an unsolved task. In recent years, the most promising results in intra-abdominal assessment of intestinal perfusion have been demonstrated using near-infrared fluorescence (NIR) technology with indocyanine green (ICG) [2–4]. This method provides a full field of view of organs perfusion inside the abdominal cavity in real time. Since only a digital camera and appropriate tissue illumination are required to implement this modality, it can be easily integrated into a standard laparoscope [5]. This modality is commercially available in laparoscopic imaging cameras and surgical robots for minimally invasive surgery. However, this technique requires injection of the fluorophore, and perfusion monitoring in the prolonged time scale is impossible. Therefore, search for alternative methods of intraoperative assessment of tissue perfusion inside the abdominal cavity is an urgent task [6].

Among the various techniques proposed for intraoperative perfusion visualization, the methods of multispectral/hyperspectral imaging (MSI/HSI) and laser-speckle-contrast imaging (LSCI) should be distinguished since these can be integrated with laparoscopes, as well. Currently, many different groups are developing MSI/HSI systems integrated with either endoscopic or laparoscopic optics to assess tissue parameters in clinical settings [7–11]. Recently reported compact HSI-laparoscope [12] is a good example of the system capable to quantitatively assess various tissue parameters. However, most of the experimental verifications were done either *ex vivo* or using phantoms. There are only few recent publications reporting the first trials of *in vivo* perfusion imaging of organs and/or tissues inside an abdominal cavity by using MSI-laparoscope, two of them were performed on animal models [9, 13], while Clancy et al. [10] demonstrated that MSI-laparoscope can derive quantitative measures of oxygen saturation in human tissue during colorectal resection. However, perfusion assessment inside the abdominal cavity is always strongly affected by motion artifacts caused by peristalsis and breathing. To correct these artifacts, video frames should be recorded at the rate higher than 30 frames per second [10], which requires high light power in each spectral band. Consequently, available data are currently limited, and the definition of thresholds or cut-off values, which distinguish between well- and poorly perfused tissue and correlate with anastomotic healing, is still pending [6].

Similarly, there are few publications devoted to intra-abdominal perfusion assessment using LSCI-laparoscopes [14–18]. Again, in most studies, experimental *in vivo* testing was carried out on an animal model. First application of laparoscopic LSCI for *in vivo* blood-flow visualization in mesentery of rats and pigs was demonstrated by Zheng et al. [14]. The only study on *in vivo* imaging of organ perfusion in humans using an LSCI laparoscope was carried out by Heeman et al. [15]. However, there are more challenges in developing the LSCI-based endoscope due to the complex scattering and inevitable tissue motions in abdominal environments and/or inside the cavities [17]. Moreover, the results of the LSCI technique are ambiguous in interpretation due to multiple light scattering in biological tissue [19].

Recently, another optical modality, imaging photoplethysmography (iPPG) has been suggested as a simple and reliable tool for intraoperative visualization and contactless quantification of tissue blood perfusion [20, 21]. Like HIS/MSI and LSCI modalities, iPPG also uses conventional video camera, but in contrast to former techniques, the tissue is illuminated by green light provided by light-emitting diodes (LED). In addition, correlation-based processing of video frames synchronously recorded with electrocardiogram allows detection of tiny light modulations associated with cardiac activity against a highly variable background caused by inevitable strong tissue motion in abdominal environment thus solving challenging task of reliable and sensitive perfusion assessment in real clinical conditions. More recently, successful application of the iPPG system to visualizing and quantitative measuring the perfusion of stomach and bowel tissues during open surgery in clinical setting has been demonstrated in our group [22, 23]. It is worth noting that simultaneous intraoperative monitoring during open abdominal surgery by using iPPG and ICG revealed a high correlation in assessing the perfusion distribution along bowels by these methods [23].

The objective of this study was to develop an iPPG-based laparoscope and demonstrate in real clinical conditions its feasibility for visualization and quantitative assessment of perfusion distribution across organs or tissues inside the abdominal cavity during different minimally invasive surgeries related to oncological resection.

Materials and methods

The study was performed at the first surgical department of the North-Western District Scientific and Clinical Center named after L.G. Sokolov of the Federal Medical and Biological Agency (Saint-Petersburg, Russia) in accordance with ethical standards presented in the 2013 Declaration of Helsinki. The study plan was approved by the Ethics Committee of the North-Western District Scientific and

Clinical Center, decision No 3 of March 13, 2023 (prior of the study). All patients and/or their legal representatives provided informed consent in written form for participation in the study.

Nine patients with gastric or colorectal cancer were selected in this study as listed in Table 1. All surgical procedures were performed by board-certified laparoscopic surgeons at our Clinical Center. Maintenance of combined anesthesia during all operations was carried out according to an author's method [24], which provided the same conditions for performing different studies. During surgical treatment, we evaluated the perfusion of organs inside the abdominal space using an iPPG laparoscope at various stages of the operation to assess the limits of applicability of the developed system for intraoperative assessment of blood flow parameters. In particular, measurements were carried out when preparing a section of the intestine or colon for resection or transection, after anastomosis, or during physiological tests. Several types of surgeries were used in this study: laparoscopic gastrectomy ($n=2$), laparoscopic sigmoid colectomy ($n=5$), laparoscopic right hemicolectomy ($n=1$), and diagnostic laparoscopy ($n=1$), see Table 1. We evaluated the areas of the intestine (jejunum for gastrectomy and colon for colorectal resection) that were supposed to be used for anastomosis. The exception was one case of diagnostic laparoscopy in which it was decided to refrain from resection due to intraoperative detection of dense inflammatory infiltrate due to diverticulitis. In other cases, measurements were made at different stages of dissection of the mesentery of the intestine: initial, after dissection of the mesentery before the transection of the intestine and after the formation of the anastomosis. In one case, during resection of the sigmoid colon, we were able to carry out measurements at three stages of mesentery dissection: after high ligation of the inferior mesenteric artery, after high ligation of the inferior mesenteric vein and after complete intersection of the mesentery at the rectosigmoid level.

Photoplethysmographic laparoscopy system

In this study, we used standard laparoscopic equipment, namely an Olympus rigid 10-mm zero-degree laparoscope (model WA53000A Olympus). A powerful (50 W) light-emitting diode operating at the wavelength of 525 nm is housed in a light supply unit “Endoscopic Illuminator EFA-M LED” (EFA Medica Ltd, St. Petersburg, Russia). The light is directed to a standard laparoscopic illumination channel by using fiber optic bundle 2.5 m long and 5 mm in diameter (see Fig. 1). The laparoscope is attached to an endoscope coupler with a focal length of 25 mm and a C-mount connection on the Complementary Metal Oxide Semiconductor (CMOS) camera UI-3060CP-M-GL (Imaging Development Systems GmbH, Germany). To improve

the measurements accuracy and obtain reliable results, we recorded video of the organs and tissues inside the abdominal cavity simultaneously and synchronously with the electrocardiogram (ECG). It was done by using digital electrocardiograph (KAP-01 “Kardiotekhnika-EKG,” Incart Ltd., St. Petersburg, Russia) using a standard ECG recording in three leads, with the placement of four electrodes on the patient's limbs. To synchronize the ECG and video data in time, the signal from the camera was connected to the fourth ECG pin (sync pulse) via the camera flash synchronization port. The images were captured using the C++ software developed in our group using the software library supplied by the camera manufacturer. Video was recorded at the rate of 21 frames per second with a resolution of 752×480 pixels and continuously stored in the personal computer in which the ECG recorded at the sampling frequency of 1 kHz was stored, as well.

Before recording the video, the surgeon directed the laparoscope inside the abdominal cavity so that the organ or tissue to be assessed for perfusion distribution were inside the field of view. The laparoscope was then fixed on a tripod to reduce the impact of motion artifacts.

Data processing

After being recorded and saved in the computer, video frames and ECG were processed offline by using custom software implemented on the MATLAB® platform (MathWorks Inc., Natick, Massachusetts). The total time required to process the recorded data and display the perfusion distribution on the screen did not exceed three minutes. The dynamics of the perfusion index was assessed in every small region of interest (ROI) sizing 2×2 pixels, which corresponds to about $40 \times 40 \mu\text{m}$ at the tissue, by the algorithm described in detail in our previous papers [22, 23]. In brief, at the first step, we minimize inevitable motion artifacts compensating for the displacement of separate parts of the digital image using sectorial optical flow algorithm [25]. Then, a photoplethysmographic (PPG) waveform was calculated as frame-by-frame evolution of the average pixel value in every ROI throughout the chosen time interval for analysis. To compensate for the inhomogeneity of tissue illumination, the ratio of the alternating component (AC) of the PPG waveform modulated at the heartbeat frequency and slowly varying (DC) component (AC/DC ratio) was calculated. The time borders for each heartbeat were determined using the R-peaks of the synchronously recorded ECG. Thereafter, a mean PPG pulse was calculated by averaging the waveforms of 15 subsequent heartbeats. Finally, a parameter called an amplitude of the pulsatile component (APC) was calculated as the difference between the maximal and minimal values of the mean PPG pulse. The parameter APC was coded in pseudo colors and its spatial distribution was overlaid with the image of the tissue under study. Physiologically, it indicates

Table 1 Patient and surgery characteristics

#	Age, year	Sex	Diagnosis	Surgery	Comorbidities
1	73	F	Sigmoid colon cancer T3N0M0	Laparoscopic sigmoid colon resection (D3 lymph nodes dissection, reconstruction: sigmo-rectoanastomosis with circular stapler 29 mm)	Hypertension—3; Risk of cardiovascular complications—4. Coronary heart disease; Coronary artery disease; Chronic heart failure—2; Type 2 diabetes mellitus; Kidney cysts
2	68	F	Gastric cancer T4aN0M0	Laparoscopic distal gastrectomy (D2 lymph nodes dissection, reconstruction: Roux-en-Y)	Coronary heart disease; Coronary artery disease; Arterial hypertension—2; Bronchial asthma; Concretion of the left kidney; Diverticulosis of the colon
3	56	M	Sigmoid colon cancer T4aN0M0	Laparoscopic sigmoid colon resection	No chronic diseases
4	46	F	Diverticular disease	Diagnostic laparoscopy (no reconstruction)	Liver steatosis; Chronic calculous cholecystitis; Risk of cardiovascular complications—3; Hypertension—1; Arterial hypertension—2; Uterine adenomyosis; Cervical cysts
5	73	F	Sigmoid colon cancer T4aN0M0	Laparoscopic sigmoid colectomy (D3 lymph nodes dissection, reconstruction: sigmorectoanastomosis with circular stapler 29 mm)	Chronic calculous cholecystitis; Diverticulosis of the colon; Chronic internal hemorrhoids; Chronic anemia; Bilateral pycloectasia; Hypertension—2; Arterial hypertension—3; Risk of cardiovascular complications—3
6	58	F	Gastric cancer T1aN0M0	Laparoscopic total gastrectomy (lymph nodes dissection D1 +, reconstruction: Roux-en-Y)	Diaphragmatic hernia—1; Catarrhal reflux-esophagitis; Diverticulosis of the sigmoid colon; Epithelial formations of the colon; Chronic hemorrhoids; Bilateral cystic fibrinous mastopathy
7	47	M	Sigmoid colon cancer T2N1aM0	Laparoscopic sigmoid colon resection (D3 lymph nodes dissection, reconstruction: sigmorectoanastomosis with circular stapler 29 mm)	No chronic diseases
8	62	M	Ascending colon cancer T2N0M0	Laparoscopic right hemicolectomy (D2 lymph nodes dissection, reconstruction: side to side ileotransversostomy with linear stapler)	Coronary heart disease; Atherosclerotic atherosclerosis; Hypertension—2; Colon polyps
9	63	M	Sigmoid colon cancer T2N0M0	Laparoscopic sigmoid colectomy (D3 lymph nodes dissection, reconstruction: sigmorectoanastomosis with circular stapler 29 mm)	Hypertension—2; Arterial hypertension—2; Risk of cardiovascular complications—3; Cerebrovascular disease; Degenerative disease of the spine; Dorsopathy of the cervical and lumbosacral regions

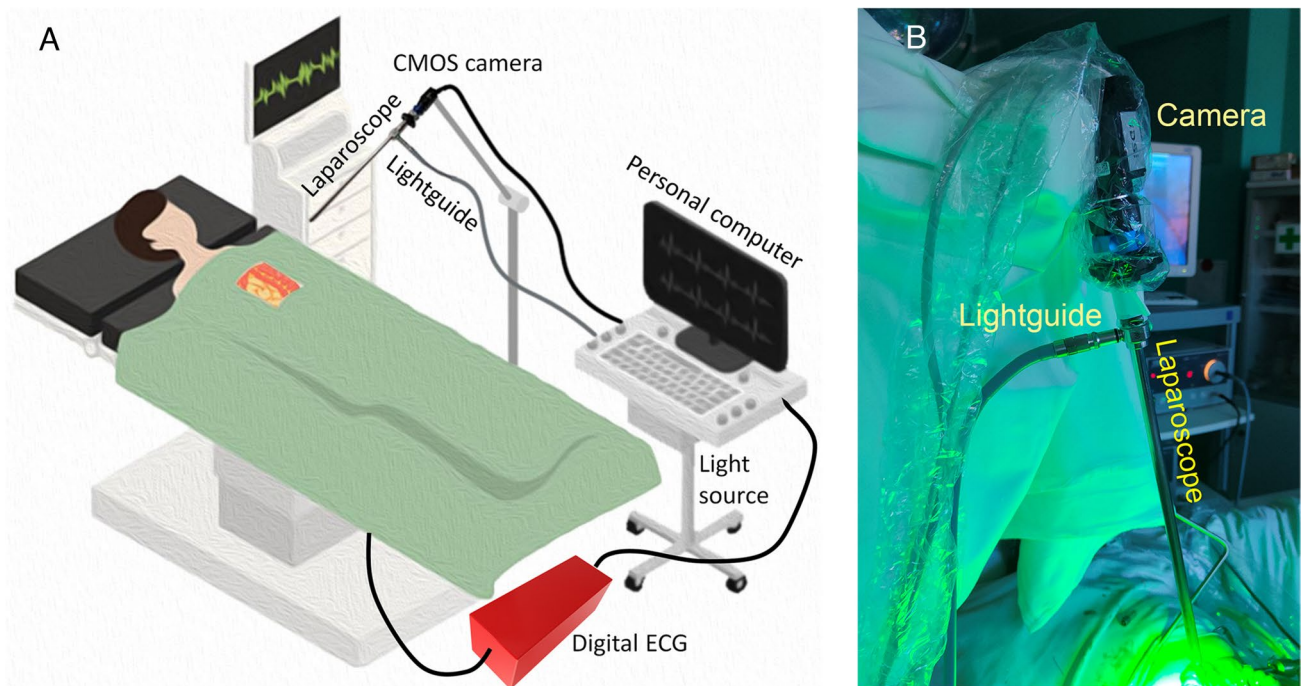


Fig. 1 The photoplethysmographic laparoscopy system developed in this study. **A** Layout of the system consisting of five major sub-systems: a rigid laparoscope, a digital camera with a Complementary Metal–Oxide–Semiconductor (CMOS) matrix, a light source, a

digital electrocardiograph (ECG), and a personal computer for data acquisition, processing, and displaying results. **B** Photograph of the system shortly before taking the intra-abdominal measurements

changes in arterial blood volume due to their pulsating nature: the greater variations of the vessels diameter regulated by the arterial tone, the higher amplitude of pulsations, i.e., APC [26, 27]. As known, this parameter represents the tone of the blood supply vessels [26] and, consequently, its map displays spatial distribution of the perfusion index.

Statistical analysis

Basic statistics were used to analyze the results. Statistical analysis of the data was performed in the MATLAB® software. The significance level was set to $p = 0.05$.

Results

Several comparative tests were performed to demonstrate feasibility of the proposed laparoscopic iPPG system to assess the perfusion of organs inside the abdominal cavity during different intestinal surgeries of the nine patients.

Changes in tissue perfusion caused by arterial clamping

Clamping of vessels feeding damaged organs should lead to a decrease in their perfusion. Intra-abdominal perfusion imaging using our iPPG laparoscope during the surgery

of laparoscopic resection of the sigmoid colon in patient #3 experimentally confirmed this assumption as shown in Fig. 2. Comparing the spatial distribution of perfusion before and after clamping and subsequent ligation of the feeding artery, a significant decrease in perfusion can be observed. The average perfusion index decreased from $1.84 \pm 0.61\%$ in Fig. 2A to $0.33 \pm 0.11\%$ in Fig. 2B; $p < 0.001$. The reaction to the artery ligation certainly depends on the individual characteristics of the collateral blood supply. In this particular case, ligation of the artery had a significant effect on the perfusion reduction, which should alert the surgeon to the diminished possibilities of perfusion compensation due to collaterals for this anatomic zone.

Another example demonstrating the potential of the iPPG laparoscope for quantifying perfusion is shown in Fig. 3, where the distribution of the perfusion index before and after clamping of the feeding artery is compared during laparoscopic sigmoid colon resection for patient #7. In this case, intra-abdominal assessment of the perfusion index of the sigmoid colon before any clamping (Fig. 3A) also demonstrated significantly higher perfusion compared to when both the feeding artery and venous vessels were clamped (Fig. 3B): $2.09 \pm 1.01\%$ versus $0.97 \pm 0.24\%$; $p = 0.02$.

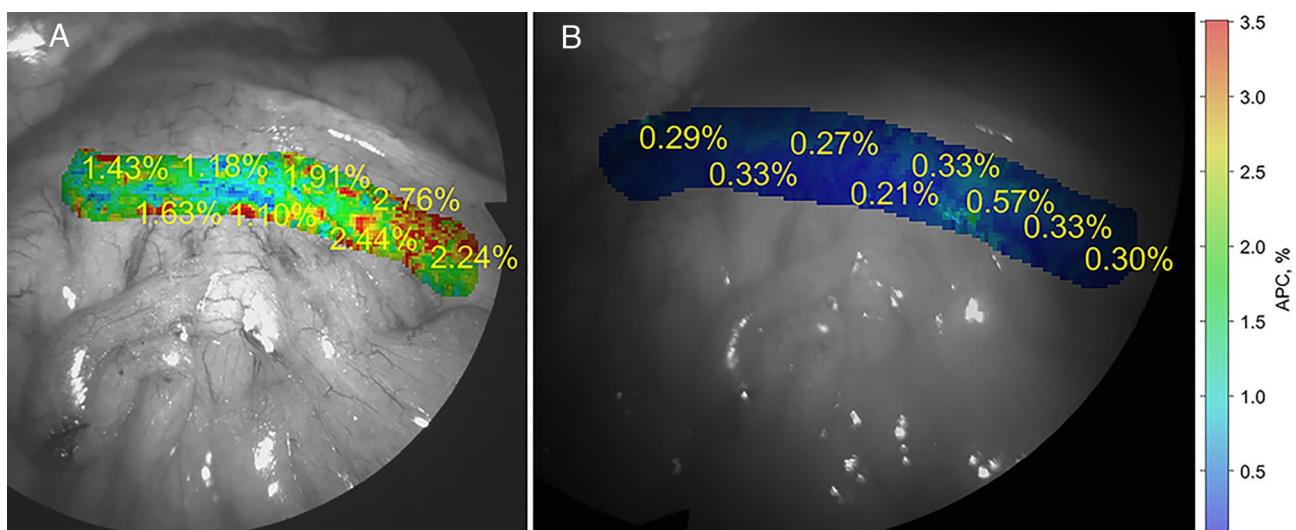


Fig. 2 Perfusion distribution in organs of patient #3 with the diagnosis of sigmoid colon cancer. Surgery: laparoscopic sigmoid colon resection. **A** Distribution of colon perfusion before any impact to abdominal organs. **B** Colon perfusion after dissection of colon mes-

entery and ligation of the feeding artery. The color scale of the index perfusion is the same for both panels and shown in the right (Color figure online)

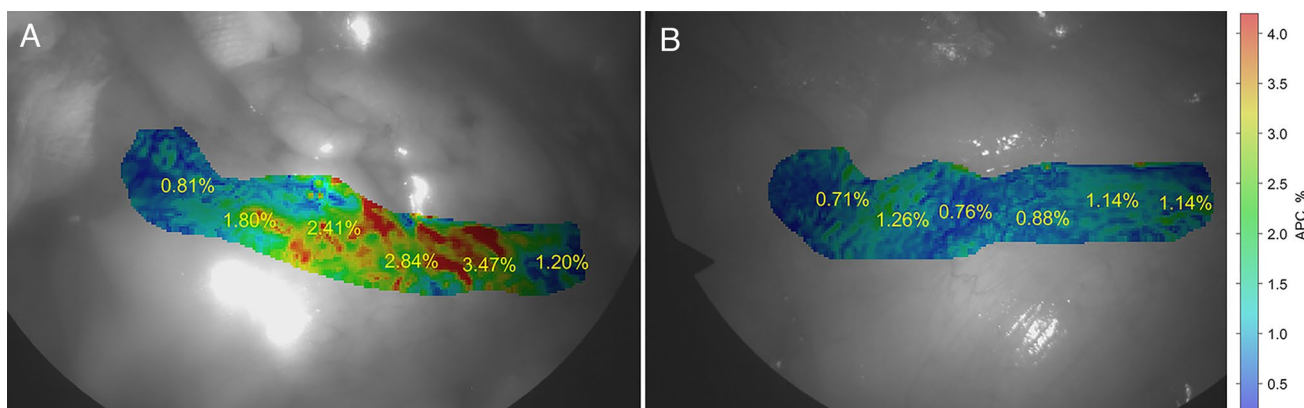


Fig. 3 Perfusion distribution in organs of patient #7 with the diagnosis of sigmoid colon cancer. Surgery: laparoscopic sigmoid colon resection. **A** Distribution of colon perfusion before any clamping. **B**

Colon perfusion after clamping both the feeding artery and venous vessels. The color scale of the index perfusion is the same for both panels and shown in the right (Color figure online)

Perfusion after anastomosis formation

With the help of our iPPG laparoscope, the initial distribution of perfusion in the intestine intended for anastomosis was compared with that yielded after anastomosis formation. All measurements were carried out inside the abdominal cavity. A typical example of visualization and quantification of perfusion during laparoscopically assisted gastrectomy is shown in Fig. 4. As can be seen from Fig. 4A, before the start of intestinal mobilization, there is a fairly uniform distribution of perfusion along the esophagus with average perfusion index of $2.0 \pm 0.3\%$. However, after the anastomosis formation (Fig. 4B),

intestinal perfusion increased significantly to $3.4 \pm 0.7\%$, $p < 0.001$. At the same time, the index of esophageal perfusion was at an even higher level of $5.3 \pm 1.2\%$, $p < 0.001$. The red dashed line in Fig. 4B indicates the location of the anastomosis suture.

Nevertheless, increase in intestinal perfusion after anastomosis formation shown in Fig. 4 is not uniquely observed dynamics. Evaluation of organs perfusion in the other four surgical cases showed that after anastomosis, perfusion in the intestine can change according to any scenario: increase (see Supplementary Fig. S1), decrease (see Supplementary Fig. S2), or remain at the level assessed before the anastomosis (see Supplementary Figs. S3 and S4).

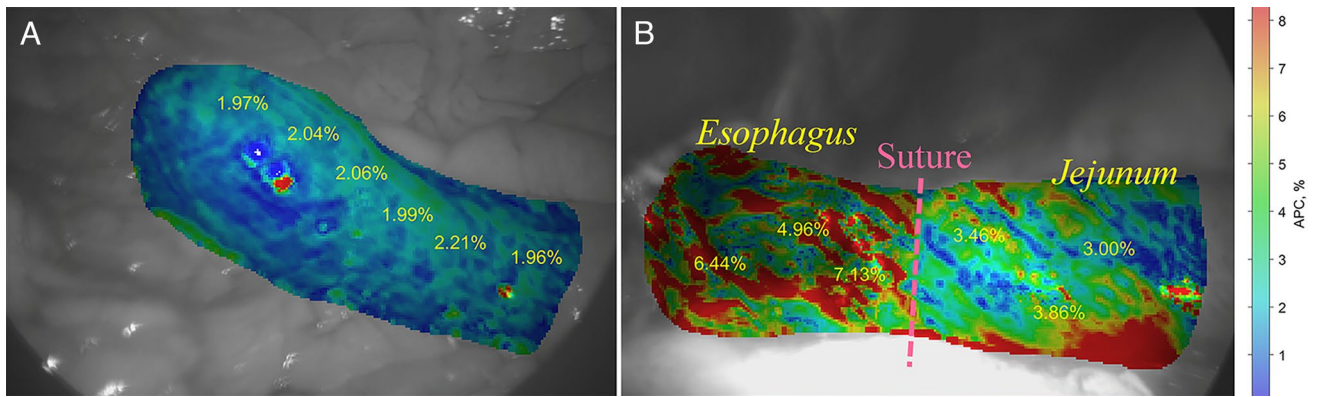


Fig. 4 Perfusion distribution in organs of patient #6 with the diagnosis of gastric cancer. Surgery: laparoscopic total gastrectomy. **A** Jejunum perfusion prior to any impact. The distribution of perfusion through the intestine is fairly uniform. **B** Perfusion after the anasto-

mosis formation. Compared to the basal recording, the perfusion of the jejunum increased significantly, and the perfusion of the esophagus (to the left of the suture) increased even more. The color scale of the index perfusion is the same for both panels (Color figure online)

Changes in tissue perfusion due to functional test

In the case of laparoscopically assisted anterior rectal resection, a physiological test was performed to assess changes in tissue perfusion due to an increase in the patient's blood pressure. After mesenteric resection, we started intra-abdominal recording of sigmoid colon images, which lasted five minutes. At the 50th second of recording, the patient was injected with norepinephrine at a rate of 3.3 $\mu\text{g}/\text{min}$. The distribution of the perfusion index before the norepinephrine injection when the blood pressure was 93/51 mmHg is shown in Fig. 5A. Two minutes after the introduction of vasoconstrictor, the pressure increased to 103/59 mmHg and the perfusion distribution at this moment is shown in Fig. 5B. As one can see, the increase in blood pressure significantly changed the intestinal perfusion: it increased in the

left part of the intestine, and on the contrary, decreased in the right part. This is proof that the iPPG laparoscope allows both visualization and quantitative assessment of organ perfusion during laparoscopic operations. Yellow dashed lines in Fig. 5 indicate location of the steepest perfusion gradient. Therefore, the proposed method is sensitive to fluctuations in perfusion parameters and demonstrates their changes both during surgical manipulations and with the introduction of vasoactive substances.

Reproducibility of perfusion assessment

Study of the reproducibility of visualization and quantitative assessment of perfusion inside abdominal cavity was carried out on three patients. Figure 6 shows the distribution of the perfusion index in the intestine and stomach after

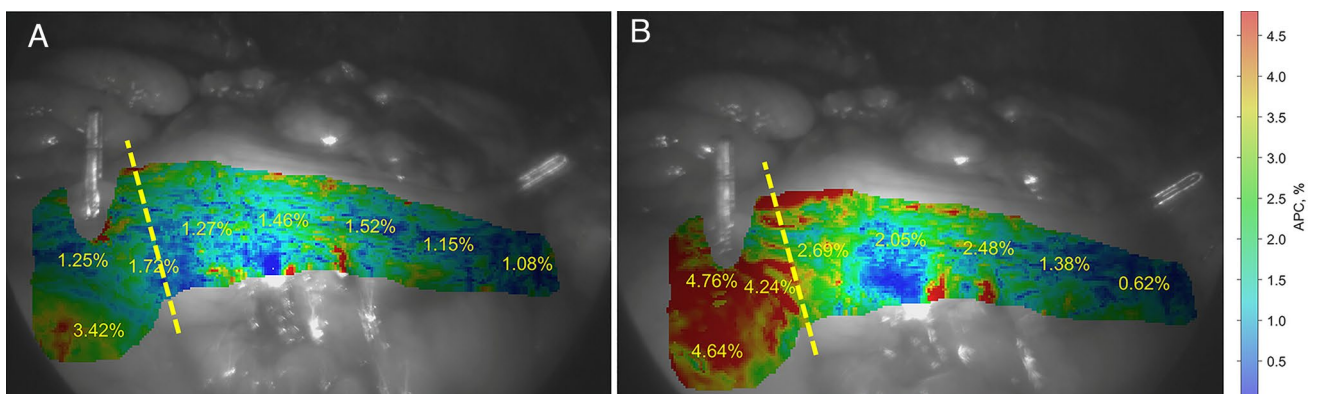


Fig. 5 Perfusion distribution in organs of patient #1 with the diagnosis of sigmoid colon cancer. Surgery: sigmoid colon resection. Sigmoid colon perfusion after mesenteric dissection and ligation the inferior mesenteric artery and vein. Pharmacological test: Change of the blood perfusion distribution due to norepinephrine injection. **A**

Before norepinephrine (blood pressure 93/51 mmHg). **B** Two minutes after injection (blood pressure 103/59 mmHg). Location of the steepest perfusion gradient is indicated by yellow dashed line. The color scale of the index perfusion is the same for both panels (Color figure online)

anastomosis in the case of laparoscopic sigmoid colectomy (patient #9). As seen, both organs are perfused at a comparable level, and perfusion is distributed fairly evenly across the anastomosis. No significant changes in perfusion were observed during seven minutes of continuous recording despite a significant change of the topology of organs viewed by the laparoscope in the course of measurements as can be easily seen comparing the photographs A and B in Fig. 6. Red dashed lines in Fig. 6 indicate the location of the staple line in the anastomosis.

The dynamics of perfusion changes for patient #9 is shown in more detail in Fig. 7, where box plots represent perfusion dispersion across the anastomosis, measured every 10 s. Relatively small size of boxes in Y-direction

reflects the uniformity of the spatial distribution of the perfusion. An example of continuous long-term (7 min) visualization of perfusion dynamics across the anastomosis is shown in Supplementary Video shot inside abdominal cavity.

More examples of the reproducibility tests are given in Supplementary Figs. S5 and S6. While in Fig. 6 we have shown the repeatability in time of homogeneous perfusion of anastomosed organs, Figs. S5 and S6 illustrate the reproducibility in time of the assessed spatial perfusion gradient across an intestine. No statistically significant difference in the location of the perfusion gradient was revealed during 40 min of measurements in the case of patient #4 (Fig. S5), as well as during 4 min for patient #8 (Fig. S6).

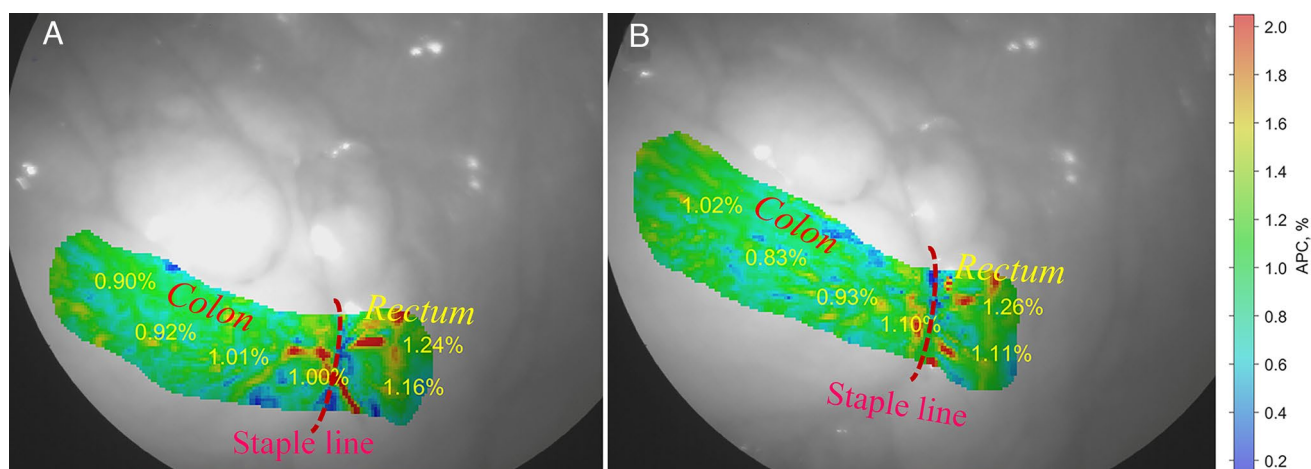
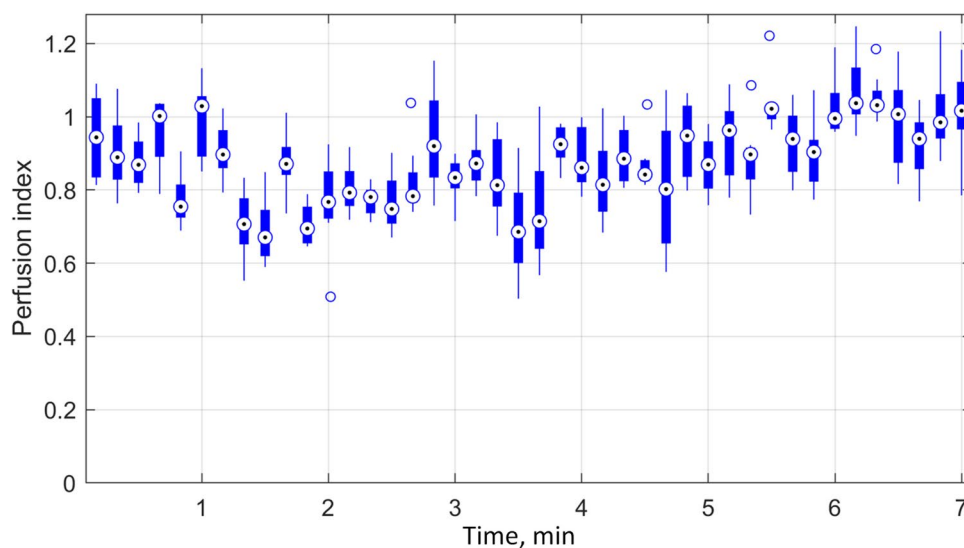


Fig. 6 Perfusion distribution in organs of patient #9 with the diagnosis of sigmoid colon cancer. Surgery: Laparoscopic sigmoid colectomy with sigmorectoproctostomy reconstruction. Checking the repeatability of the perfusion visualization during prolonged continuous measurements after the anastomosis formation. **A** Perfusion dis-

tribution measured at the beginning of recording. The perfusion index in both organs is the same. **B** Perfusion index after 7 minutes of recording. Despite a significant change in the field of view of the laparoscope, the distribution of perfusion in the connected organs remains quantitatively unchanged (Color figure online)

Fig. 7 Evolution of the index perfusion during of a prolonged continuous monitoring of the anastomosis blood supply inside the abdominal cavity for patient #9 with the diagnosis of sigmoid colon cancer



Discussion

Our study aims to demonstrate for the first time the successful implementation of the laparoscopic iPPG system to support minimally invasive surgery in clinical setting. Its use proved to be safe and feasible in all patients. In this study, we used a standard laparoscope equipped with a monochrome CMOS camera to acquire intra-abdominal images of organs under study. We have developed an algorithm that allows us to quantify the spatial distribution of the perfusion index under conditions of significant dynamic changes in the topology of the organ under study. The main distinguishing feature of our algorithm is the correlation processing of video data recorded synchronously with the ECG. With the developed laparoscopic perfusion imager, we were able to detect both compromised intestinal perfusion and the distribution of perfusion across the organs after anastomosis. In addition, the possibility of long-term continuous quantification of perfusion distribution has been demonstrated.

Assessment of the spatial gradient of blood supply to the impacted organs is one of the most important factors influencing intraoperative decision-making. The parameters of blood flow can be influenced by numerous factors, the indicators of which are noticeably varying during a single surgery. However, it is the difference in the level of blood-flow parameters in different parts of a colon (or another organ) that gives the key to assessing the state of the organ's perfusion in terms of surgically significant events. In our study, we have demonstrated for the first time a phenomenon of pharmacological enhancement of perfusion gradients. In particular, systemic administration of norepinephrine lead to an increased gradient between well and poorly perfused areas of the colon due to an increased systemic arterial pressure. Notably that all perfusion assessments were carried out inside the abdominal cavity during laparoscopic surgeries in the operations theater. It is a reliable assessment of the perfusion gradient, which is the main criterion used by the surgeon when choosing a resection line. Nevertheless, the operation involves many different stages, in particular, no less important is the control of perfusion in the anastomosed organs, during which an adequate intraoperative assessment of intestinal perfusion is required to ascertain the viability of the newly formed anastomosis. As we have demonstrated, the iPPG-laparoscope successfully copes with this task.

The main advantage of the developed laparoscopic system is the possibility to easily and continuously acquire new quantitative images during the surgery, representing the perfusion distribution along organs. It should be especially emphasized that the system allows for a quantitative

assessment of the perfusion gradient inside the abdominal cavity in challenging conditions when different areas of the organs are displaced both relative to each other in arbitrary directions, and relative to the entrance pupil of the laparoscope.

Current limitation of the laparoscopic perfusion imager is an offline data processing. However, in the nearest future we will develop an advanced data processing algorithm that will allow continuous visualizing and quantifying perfusion in real time.

Conclusion

Imaging photoplethysmography, improved due to correlation processing of video data synchronously recorded with an ECG, can be easily combined with a standard laparoscope thus allowing intra-abdominal visualization and quantitative assessment of perfusion distribution. This is a new technology that holds great potential for clinical applications in minimally invasive surgery. Our current study is an important step toward the clinical implementation of iPPG-laparoscope for minimally invasive surgery.

Supplementary Information The online version contains supplementary material available at <https://doi.org/10.1007/s00464-023-10506-y>.

Acknowledgements The authors like to thank Mr. Vladimir Artemov from the EFA Medica Ltd for the fruitful discussions and his crucial notes.

Author contributions VK and AK drafted the study plan. AK and VZ developed the conceptual framework for iPPG video analyses, designed and manufactured the technical setup as well as developed the data processing software. VK and AL carried out the surgical interventions. CK provided anesthesia for patients and physiological tests. AK and VK analyzed the experimental data. AK drafted the manuscript. VZ and AK prepared the figures. All authors critically reviewed and approved the manuscript.

Funding The study was carried out with the financial support of the Russian Science Foundation (Grant No. 21-15-00265) in terms of the manufacture of the experimental equipment, software development, and data processing and analysis. Research planning, patient preparation, and surgical interventions were carried out with the financial support of the Government of the Russian Federation for the state support of scientific research carried out under the supervision of leading scientists (Agreement No. 075-15-2022-1110).

Declarations

Disclosures Dr. Victor A. Kashchenko, Dr. Alexander V. Lodygin, Dr. Konstantin Yu. Krasnoselsky, Valery V. Zaytsev, and Dr. Alexei A. Kamshilin have no conflicts of interest or financial ties to disclose.

References

1. Urbanavičius L, Pattyn P, de Putte D, Van VD (2011) How to assess intestinal viability during surgery: a review of techniques.

- World J Gastrointest Surg 3:59–69. <https://doi.org/10.4240/wjgs.v3.i5.59>
2. Miyashiro I, Kishi K, Yano M, Tanaka K, Motoori M, Ohue M, Ohigashi H, Takenaka A, Tomita Y, Ishikawa O (2011) Laparoscopic detection of sentinel node in gastric cancer surgery by indocyanine green fluorescence imaging. *Surg Endosc* 25:1672–1676. <https://doi.org/10.1007/s00464-010-1405-3>
 3. Park S-H, Park H-M, Baek K-R, Ahn H-M, Lee IY, Son GM (2020) Artificial intelligence based real-time microcirculation analysis system for laparoscopic colorectal surgery. *World J Gastroenterol* 26:6945–6962. <https://doi.org/10.3748/wjg.v26.i44.6945>
 4. Hellan M, Spinoglio G, Pigazzi A, Lagares-Garcia JA (2014) The influence of fluorescence imaging on the location of bowel transection during robotic left-sided colorectal surgery. *Surg Endosc* 28:1695–1702. <https://doi.org/10.1007/s00464-013-3377-6>
 5. Diana M, Agnus V, Halvax P, Liu Y-Y, Dallemagne B, Schlagowski A-I, Geny B, Diemunsch P, Lindner V, Marescaux J (2015) Intraoperative fluorescence-based enhanced reality laparoscopic real-time imaging to assess bowel perfusion at the anastomotic site in an experimental model. *Br J Surg* 102:e169–e176. <https://doi.org/10.1002/bjs.9725>
 6. Chalopin C, Pfahl A, Köhler H, Knospe L, Maktabi M, Unger M, Jansen-Winkel B, Thieme R, Moulla Y, Mehdorn M, Sucher R, Neumuth T, Gockel I, Melzer A (2022) Alternative intraoperative optical imaging modalities for fluorescence angiography in gastrointestinal surgery: spectral imaging and imaging photoplethysmography. *Minim Invasive Ther Allied Technol* 31:1–11. <https://doi.org/10.1080/13645706.2022.2164469>
 7. Schols RM, Bouvy ND, van Dam RM, Stassen LPS (2013) Advanced intraoperative imaging methods for laparoscopic anatomy navigation: an overview. *Surg Endosc* 27:1851–1859. <https://doi.org/10.1007/s00464-012-2701-x>
 8. Han Z, Zhang A, Wang X, Sun Z, Wang MD, Xie T (2016) In vivo use of hyperspectral imaging to develop a noncontact endoscopic diagnosis support system for malignant colorectal tumors. *J Biomed Opt* 21:16001. <https://doi.org/10.1117/1.JBO.21.1.016001>
 9. Wakabayashi T, Barberio M, Urade T, Pop R, Seyller E, Pizzicannella M, Mascagni P, Charles A-L, Abe Y, Geny B, Baiocchi A, Kitagawa Y, Marescaux J, Felli E, Diana M (2021) Intraoperative perfusion assessment in enhanced reality using quantitative optical imaging: an experimental study in a pancreatic partial ischemia model. *Diagnostics* 11:93. <https://doi.org/10.3390/diagnostics11010093>
 10. Clancy NT, Soares AS, Bano S, Lovat LB, Chand M, Stoyanov D (2021) Intraoperative colon perfusion assessment using multispectral imaging. *Biomed Opt Express* 12:7556–7567. <https://doi.org/10.1364/BOE.435118>
 11. Pfahl A, Köhler H, Thomaßen MT, Maktabi M, Bloße AM, Mehdorn M, Lyros O, Moulla Y, Niebisch S, Jansen-Winkel B, Chalopin C, Gockel I (2022) Video: clinical evaluation of a laparoscopic hyperspectral imaging system. *Surg Endosc* 36:7794–7799. <https://doi.org/10.1007/s00464-022-09282-y>
 12. Thomaßen MT, Köhler H, Pfahl A, Stelzner S, Mehdorn M, Thieme R, Jansen-Winkel B, Gockel I, Chalopin C, Moulla Y (2023) In vivo evaluation of a hyperspectral imaging system for minimally invasive surgery (HSI-MIS). *Surg Endosc* 37:3691–3700. <https://doi.org/10.1007/s00464-023-09874-2>
 13. Urade T, Felli E, Barberio M, Al-Taher M, Felli E, Goffin L, Agnus V, Ertorre GM, Marescaux J, Mutter D, Diana M (2021) Hyperspectral enhanced reality (HYPER) for anatomical liver resection. *Surg Endosc* 35:1844–1850. <https://doi.org/10.1007/s00464-020-07586-5>
 14. Zheng C, Lau LW, Cha J (2018) Dual-display laparoscopic laser speckle contrast imaging for real-time surgical assistance. *Biomed Opt Express* 9:5962–5981. <https://doi.org/10.1364/BOE.9.005962>
 15. Heeman W, Dijkstra K, Hoff C, Koopal S, Pierie J-P, Bouma H, Boerma EC (2019) Application of laser speckle contrast imaging in laparoscopic surgery. *Biomed Opt Express* 10:2010–2019. <https://doi.org/10.1364/BOE.10.002010>
 16. Potapova EV, Seryogina ES, Dremine VV, Stavtsev DD, Kozlov IO, Zherebtsov EA, Mamoshin AV, Ivanov YV, Dunaev AV (2020) Laser speckle contrast imaging of blood microcirculation in pancreatic tissues during laparoscopic interventions. *Quantum Electron* 50:33–40. <https://doi.org/10.1070/qel17207>
 17. Guo Y, Weng Y, Zhang Y, Tong S, Liu Y, Lu Z, Miao P (2023) Random matrix-based laser speckle contrast imaging enables quasi-3D blood flow imaging in laparoscopic surgery. *Biomed Opt Express* 14:1480–1493. <https://doi.org/10.1364/BOE.483655>
 18. Heeman W, Wildeboer ACL, Al-Taher M, Calon JEM, Stassen LPS, Diana M, Derikx JPM, van Dam GM, Boerma EC, Bouvy ND (2023) Experimental evaluation of laparoscopic laser speckle contrast imaging to visualize perfusion deficits during intestinal surgery. *Surg Endosc* 37:950–957. <https://doi.org/10.1007/s00464-022-09536-9>
 19. Kazmi SMS, Faraji E, Davis MA, Huang Y-Y, Zhang X, Dunn AK (2018) Flux or speed? Examining speckle contrast imaging of vascular flows. *Biomed Opt Express* 6:2588–2608. <https://doi.org/10.1364/BOE.6.002588>
 20. Mamontov OV, Shcherbinin AV, Romashko RV, Kamshilin AA (2020) Intraoperative imaging of cortical blood flow by camera-based photoplethysmography at green light. *Appl Sci* 10:6192. <https://doi.org/10.3390/app10186192>
 21. Kukul I, Trumpp A, Plötze K, Rost A, Zaunseder S, Matschke KE, Rasche S (2020) Contact-free optical assessment of changes in the chest wall perfusion after coronary artery bypass grafting by imaging photoplethysmography. *Appl Sci* 10:6537. <https://doi.org/10.3390/app10186537>
 22. Kamshilin AA, Zaytsev VV, Lodygin AA, Kashchenko VA (2022) Imaging photoplethysmography as an easy-to-use tool for monitoring changes in tissue blood perfusion during abdominal surgery. *Sci Rep* 12:1143. <https://doi.org/10.1038/s41598-022-05080-7>
 23. Kashchenko VA, Zaytsev VV, Ratnikov VA, Kamshilin AA (2022) Intraoperative visualization and quantitative assessment of tissue perfusion by imaging photoplethysmography: comparison with ICG fluorescence angiography. *Biomed Opt Express* 13:3954–3966. <https://doi.org/10.1364/BOE.462694>
 24. Krasnoselsky KY, Salnikov VG, Shirinbekov NR, Aleksandrovich YS (2019) TIVA manager—component of control of general anesthesia. In: Abstracts of the XVIII International Euroasian Congress of Surgery and Hepatogastroenterology. 11–14 Sept 2019, Baku, Azerbaijan, pp. 330–331
 25. Kamshilin AA, Krasnikova TV, Volynsky MA, Miridonov SV, Mamontov OV (2018) Alterations of blood pulsations parameters in carotid basin due to body position change. *Sci Rep* 8:13663. <https://doi.org/10.1038/s41598-018-32036-7>
 26. Lyubashina OA, Mamontov OV, Volynsky MA, Zaytsev VV, Kamshilin AA (2019) Contactless assessment of cerebral autoregulation by photoplethysmographic imaging at green illumination. *Front Neurosci* 13:1235. <https://doi.org/10.3389/fnins.2019.01235>
 27. Volynsky MA, Mamontov OV, Osipchuk AV, Zaytsev VV, Sokolov AY, Kamshilin AA (2022) Study of cerebrovascular reactivity to hypercapnia by imaging photoplethysmography to develop a method for intraoperative assessment of the brain

functional reserve. *Biomed Opt Express* 13:184–196. <https://doi.org/10.1364/BOE.443477>

Publisher's Note Springer Nature remains neutral with regard to jurisdictional claims in published maps and institutional affiliations.

Springer Nature or its licensor (e.g. a society or other partner) holds exclusive rights to this article under a publishing agreement with the author(s) or other rightsholder(s); author self-archiving of the accepted manuscript version of this article is solely governed by the terms of such publishing agreement and applicable law.